Proceedings of the ASME 2020
14th International Conference on Energy Sustainability
ES2020
June 8-10, 2020, Denver, CO, USA

SAND2020-3105C

DRAFT

ES2020-1666

PARTICLE FLOW TESTING OF A MULTISTAGE FALLING PARTICLE RECEIVER CONCEPT: STAGGERED ANGLE IRON RECEIVER (STAIR)

Lindsey Yue[1], Nathan Schroeder, Clifford K. Ho
Sandia National Laboratories
Albuquerque, NM, USA

ABSTRACT

Falling particle receivers are an emerging technology for use in concentrating solar power systems. In this work, a staggered angle iron receiver concept is investigated, with the goals of increasing particle curtain stability and opacity in a receiver. The concept consists of angle iron-shaped troughs placed in line with a falling particle curtain in order to decrease the downward velocity of the particles and reintroduce particles from a single point, decreasing curtain spread. A particle flow test apparatus has been fabricated. The effect of staggered angle iron trough geometry, orientation, and position on the opacity and uniformity of a falling particle curtain for different particle linear mass flow rates is investigated using the particle flow test apparatus. For the baseline free falling curtain and for different trough configurations, particle curtain transmissivity is measured, and profile images of the particle curtain are taken. Particle mass flow rate and trough position affect curtain transmissivity more than trough orientation and geometry. Optimal trough position for a given particle mass flow rate can result in improved curtain stability and decreased transmissivity. However, some trough configurations have a detrimental effect on curtain stability and result in increased curtain transmissivity and/or substantial particle bouncing.

Keywords: concentrated solar power, falling particle receiver, thermal efficiency, multistage release.

INTRODUCTION

Falling particle receivers (FPR) are an emerging technology for use in concentrating solar power (CSP) systems [1]. FPRs have the potential to operate at higher temperatures than current direct-steam or molten-salt receivers, thus increasing the maximum potential operating temperature of the CSP power cycle and the solar-to-electric efficiency [2]. However, in unobstructed particle receivers, particle curtain opacity and thus curtain solar absorptance decreases with increasing curtain drop distance [3][4][5]. In this work, a staggered angle iron receiver (StAIR) concept is investigated, with the goal of increasing particle curtain opacity in a receiver.

Other concepts have been investigated for obstructing falling particle curtain flow to increase particle curtain opacity. An obstructed-flow concept featuring interconnected porous media placed in the flow path of the particle curtain had been investigated numerically [6] and experimentally [7]. The obstructed-flow concept yielded larger particle temperature increases and higher thermal efficiencies in experiments than a free falling particle curtain in the same receiver. However, technical challenges were encountered including non-uniform lateral particle mass flow and deterioration of the porous medium structure.

A multistage release concept featuring regularly spaced troughs in the path of the particle flow has also been numerically and experimentally investigated [8]. In this concept, particle fall either between the leading and back trough edge or between a trough leading edge and back wall. The number of stages required for a given particle linear mass flow rate was identified numerically for drop distances up to 6 m. Curtain opacity was compared visually from 6 m drop experiments with and without multistage release. Curtain opacity was observably higher with multistage release compared to the free fall curtain. However, optical losses and material durability were noted concerns.

In the StAIR concept presented in this work, angle iron-shaped troughs are placed in the path of the falling particle

[1] Contact author: lyue@sandia.gov

Sandia National Laboratories is a multimission laboratory managed and operated by National Technology & Engineering Solutions of Sandia, LLC, a wholly owned subsidiary of Honeywell International Inc., for the U.S. Department of Energy's National Nuclear Security Administration under contract DE-NA0003525.

curtain. Particles collect in the troughs until particles fill the trough and flow over the leading trough edge, falling again until encountering another trough or exiting the receiver. Potential benefit of the StAIR concept include: (1) particles impact on particles rather than the troughs minimizing erosion; (2) particle fall over the trough leading edge shading the troughs from direct irradiation, eliminating the need for exotic and expensive materials, (3) minimal receiver modifications are required to accommodate the StAIR concept, allowing independent optimization of receiver geometry and StAIR configuration, and (4) scalability.

A particle flow test apparatus has been fabricated to investigate the effect of staggered angle iron trough geometry, orientation, and position on the opacity and uniformity of a falling particle curtain. Trough internal angle, rotational orientation, horizontal position, and vertical position were varied for different particle mass flow rates, and particle curtain opacity was quantified for each configuration by measuring curtain opacity at a specific location below the trough. The goal of this work is to find a configuration of trough size, shape, spacing, and orientation that (1) increases curtain opacity relative to the curtain opacity with no troughs, and (2) decreases or minimizes particle bouncing and loss.

Trough vertical and horizontal position affect curtain transmissivity more than trough orientation and internal angle. Minimum trough vertical distance exists for considered particle linear mass flow rate above which troughs do not improve curtain transmissivity over the baseline while below which troughs do improve curtain transmissivity over the baseline. Trough horizontal position and, to a lesser extent, orientation affect curtain transmissivity, suggesting particle pile size and shape and the position the particle curtain impinges on the pile influence how particles exiting the trough. Curtain opacity increases (equivalent to decreased curtain spread, increased local particle volume fraction, and transmissivity decreases) with increasing trough orientation angle for troughs placed closer to the slot, suggesting larger particle piles in the troughs lead to less particle bouncing caused by less particle-to-trough contact.

1 Methodology

In this section, the test apparatus, including test rig and instrumentation will be described. Next, the equation for calculating particle curtain transmissivity is discussed. Finally, the test procedure is outlined.

1.1 Test apparatus

The test rig consists of a top hopper and particle curtain release slot. Flow through the slot is controlled using a linear actuated slide gate that adjusts to control the particle mass flow rate. The slot is 12” wide, and the slide gate can be adjusted for initial curtain thickness from 1/8” (3.18 mm) to 1/2” (12.7 mm), corresponding to linear particle mass flow rates of 1–8 kg s^{-1} m^{-1}. The top hopper and slide gate are mounted on top of a frame. The frame includes mounts for three angle iron troughs. The mounts allow the troughs to be independently adjusted horizontally, vertically, and rotationally. Particles are collected in the bottom hopper at the base of the test rig.

Instrumentation includes a Cole-Parmer® Digi-Sense Traceable® Dual-Range Light Meter mounted behind the particle curtain, which can be adjusted vertically, and two 600-watt halogen lamps, proving a light source mounted approximately 2 m directly in front of the curtain. The light meter is calibrated using a halogen light source. The light source was sized to provide several times more luminous flux to the light meter than the background ambient light. Background ambient light and the light source measured with the light meter in preliminary tests were on the order of 100 and 3000 lux, respectively. Particle mass flow rate is measured using a hopper placed on top of a Lonestar™ Sensors RSP1 Single Point Load Cell positioned directly under the slot opening. Particle linear mass flow rate is calculated by dividing particle mass flow rate by the slot width of 12”. The conceptual design with three troughs and fabricated test rig are shown in Figure 1.

(a) (b)

FIGURE 1: Particle flow test apparatus (a) conceptual design and (b) fabricated rig

Angle iron-shaped troughs consist of two aluminum pieces welded together. The leading front edge length is 3/16” thick and 2” long; and the back edge length is 1/4” thick and 8” long. The aluminum surfaces were lightly sanded using a flap wheel grinder to remove dirt and oxidation. Two sets of three troughs were fabricated for this testing: sets had the same front and back edge length with different internal angles, defined as the angle between the front and back trough edges.

Digital cameras were used to document particle curtain flow in video and still images. The video and still images are used to

qualitatively compare particle curtain trajectory, stability, and volume fraction between cases.

1.2 Curtain transmissivity

Luminous flux measurements are used to determine the particle curtain transmissivity to the light source. 'Transmissivity' is used in this work to refer to the total hemispherical transmissivity of the particle curtain over the visible radiation spectrum. The halogen light source does not have the same spectral distribution as solar radiation. The visible radiation spectrum does not include all electromagnetic wavelengths, including short wavelengths in the infra-red region, which constitute a substantial fraction of energy in solar radiation. Therefore, transmissivity values should be used comparatively within this work and should not be used to estimate total solar absorptivity of particle curtains.

A schematic depicting luminous flux from the light source and background light interacting with the particle curtain and light meter is shown in Figure 2. Particle curtain transmissivity is calculated as the ratio of luminous flux from the light source with and without the particle curtain, represented in Figure 2 as dashed and solid red/thick lines, respectively. Background luminous flux is not included in the transmissivity calculation to remove the influence of potentially variable background light on transmissivity values.

Four luminous fluxes are measured to calculate particle curtain transmissivity to the light source. The background luminous flux (with no light source) is first measured with and without the particle curtain. The background luminous flux without the particle curtain is represented by all the solid blue/thin lines in Figure 2. The background luminous flux with the particle curtain is represented by the dashed blue/thin lines between the particle curtain and light meter as well as the solid blue/thin lines to the sides of the curtain. Luminous flux from both the background and light source is then measured with and without the particle curtain. The luminous flux from both the background and light source without the particle curtain is represented by the solid blue/thin and red/thick lines in Figure 2. The luminous flux from both the background and light source with the particle curtain is represented as the dashed blue/thin and red/thick lines between the particle curtain and the light meter as well as the solid blue/thin lines to the sides of the curtain. Transmissivity is then calculated according to the following equation:

$$\tau = \frac{q''_{\mathrm{c,lights}} - q''_{\mathrm{c,nolights}}}{q''_{\mathrm{lights}} - q''_{\mathrm{nolights}}} \quad (1)$$

where $q''_{\mathrm{c,lights}}$ is the luminous flux measured with the curtain and light source (dashed blue/thin and red/thick lines in Figure 2); $q''_{\mathrm{c,nolights}}$ is the background luminous flux measured with the curtain but with no light source (dashed blue/thin lines); q''_{lights} is the luminous flux measured with the light source and no curtain (solid blue/thin and red/thick lines); and q''_{nolights} is the background luminous flux measured without the light source or curtain (solid blue/thin lines).

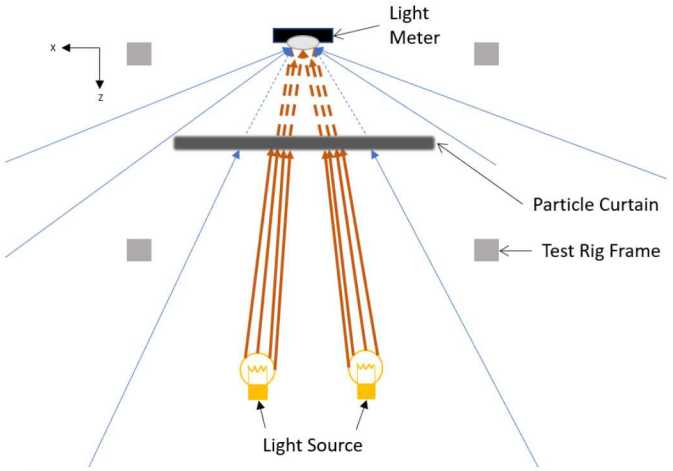

FIGURE 2: Luminous flux from the light source (red/thick lines) and background light (blue/thin lines) interacting with the particle curtain and light meter

1.3 Test procedure

The following test procedure applies to each investigated configuration unless otherwise specified. The linear actuator distance is set to result in the desired particle mass flow rate; and particles are loaded into the top hopper. The particle mass flow rate is measured without troughs before and after testing daily using the load cell. After the initial particle mass flow rate measurement, troughs are positioned. Trough position is determined using rulers mounted on the test rig, a weighted float in line with the top hopper slot opening, and preliminary flow testing for fine tune adjustment. The light meter is positioned relative to the slot and/or the bottom of the vertex of the trough above.

The light meter begins recording data before the light source is turned on and before the slide gate is opened to obtain the first background luminous flux measurement with no light source and no particle curtain. The slide gate is then opened, and the particle curtain falls until steady flow is achieved to obtain the second background luminous flux reading with the particle curtain and no light source. The slide gate is then closed. This process is repeated with the light source turned on to obtain the two luminous flux readings with the light source with and without the curtain. In tests involving two troughs, the vertical position of the second trough relative to the location the particle curtain impinges on the trough is determined using preliminary flow tests.

2 Results and discussion

Four experimental campaigns have been performed and the results will be presented in the following sections. Results include trough and light meter position, calculated transmissivity values, and images of exemplary cases. Baseline measurements of curtain transmissivity for various drop distances are first presented. Then, results with a single trough with internal angle

90° for varying trough orientation, horizontal and vertical trough position, and particle mass flow rate are presented. Next, the results from the same campaign repeated with a single trough with internal angle 120° are presented. Lastly, results from tests with two troughs both with 90° internal angle are presented and discussed. All results with troughs are compared to the baseline measurements.

Trough orientation is defined by the angle between the trough leading edge and horizontal (xz plane shown in Figure 1a and Figure 2) which was varied from 35–65° for tests with the single 90° internal angle trough and 25–45° for tests with the single 120° internal angle trough. Three vertical trough positions were considered: the trough vertex positioned 12”, 24”, and 36” inches below the slot opening. Trough horizontal position was determined by aligning the trough vertex parallel to the x axis directly below the particle curtain release slot, and then the trough horizontal position was varied from 0 to +2” forward from the nominal position. Positions more forward or back of this range were not considered. We observed in preliminary testing particle curtains that impinged on the front of the particle pile (horizontal positions behind the nominal position) or on the exposed back edge of the trough (horizontal positions more that 2” forward of the nominal position) resulted in substantial particle bouncing and increases transmissivity.

The light meter was placed 12” below the vertex of the trough, corresponding to 24”, 36”, and 48” inches below the slot (neglecting the thickness of the trough walls). For particle mass flow rate, two particle release slot depths were considered: 1/4” and 1/2”, corresponding to 0.59–0.62 and 1.5–1.8 kg s^{-1}, respectively, or 1.9–2.1 and 5.0–5.8 kg s^{-1} m^{-1}, respectively. A range of particle mass flow rates is associated with a single slot depth due to the variability between linear actuator length each time the length is adjusted. Both the slot depth setting and the measured particle mass flow rate will be reported for clarity.

Particle mass flow rates measured for the same slot depth between linear actuator adjustments are statistically different. Five particle mass flow rate measurements were taken over the course of several days for a slot depth of 1/4” without adjusting the linear actuator. The average of those measurements is 0.60 with standard deviation 0.01 kg s^{-1}. After adjusting the linear actuator away from and back to 1/4”, three measurements were taken with average 0.624 with standard deviation 0.002 kg s^{-1}. For a slot depth of 1/4” the different between linear actuator adjustments is assumed small enough to be neglected. The different between linear actuator adjustments for a slot depth of 1/2” is larger, because particle mass flow rate increases exponentially with increasing slot depth [9]. Future work will include an investigation to the sensitive of results to variable particle mass flow rates for slot depth 1/2”.

2.1 Baseline results

For slot depths of 1/4” and 1/2”, the particle curtain transmissivity was measured for drop distances of 12”, 24”, 36”, and 48” below the slot. An exemplary free fall particle curtain with slot depth 1/2” with indicated measurement locations is shown in Figure 3. The particle curtain moves in the negative z direction (towards the back of the test apparatus), because particles have some negative z direction velocity imparted on them when exiting the slot and coming off the end of the slide gate which is mounted a few millimeters below the slot opening. This behavior is consistent with previously observed slide gate-controlled particle curtains [9]. The bottom hopper is shown in an elevated position in the image but is moved to a lower location when the light meter is positioned at 48” below the slot so the hopper does not obstruct the light meter.

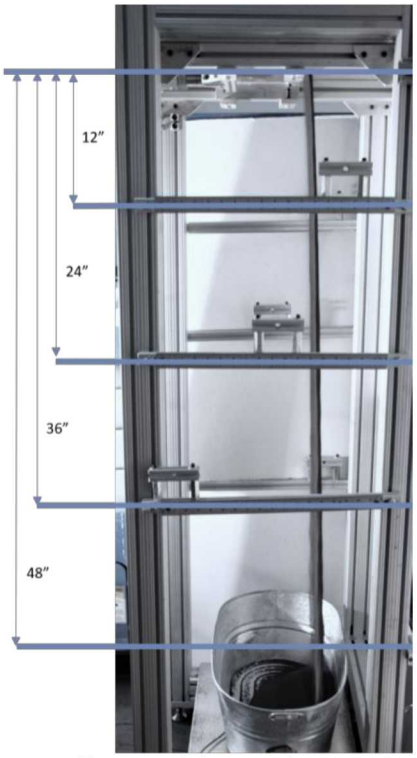

FIGURE 3: Baseline particle curtain: top hopper slot is indicated by the top line and light meter positions are indicated by the bottom four lines

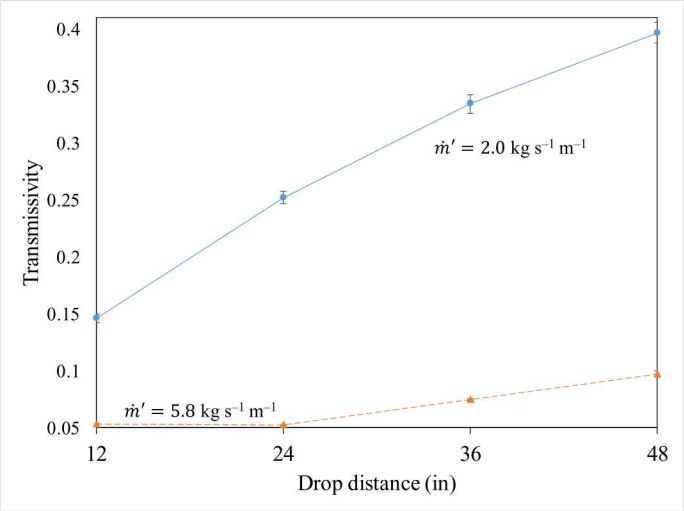

FIGURE 4: Baseline particle curtain transmissivity versus curtain drop distance for slot depths 1/4" (dashed red line and triangles) and 1/2" (solid blue line and circles); error bars represent the aggregated standard deviation of measured values

Curtain transmissivity is shown versus drop distance for slot depths of 1/4" and 1/2". Two sets of measurements for 1/2" slot depth are shown from before and after adjustment of the linear actuator distance, corresponding to particle linear mass flow rates of 5.0 and 5.8 kg s^{-1} m^{-1}. A measurement was not taken at 48" for the 5.0 kg s^{-1} m^{-1} setting. Transmissivity decreases with drop distance in agreement with previously reported observations [3][4] and simulations [5] for similar particle linear mass flow rates.

Baseline results for slot depth 1/2" indicate curtain opacity does not start significantly decreasing until the curtain has dropped 36" or more. The difference between transmissivity measurements at 24" suggests further investigation into baseline curtain behavior for given slot depths and variability between measurements is warranted. Differences in transmissivity values between cases smaller than the difference between measurements for the baseline curtain at 24" will not be considered conclusive.

For the considered mass flow rates and maximum particle curtain drop distance accommodated by the test apparatus, curtain will not fall a sufficient distance to reach a maximum transmissivity value. This indicates the test rig may not be tall enough to capture drop distances at which increases in curtain stability and particle volume fraction are more significant. Future work may include considering lower particle mass flow rates and thus, free fall curtains with more rapidly increasing particle volume fraction and decreasing opacity to better understand the distances at which troughs improve curtain transmissivity.

2.2 Single trough with 90° internal angle

An example image from a selected 90° internal angle trough test is shown in Figure 5 to illustrate the test set up. In the test shown in the figure, the trough vertex is positioned 36" below the slot (vertical position); the light meter is 12" below the trough vertex; and trough vertex is aligned with the particle curtain at the point of impingement (nominal horizontal position); and the trough is oriented at a 35°.

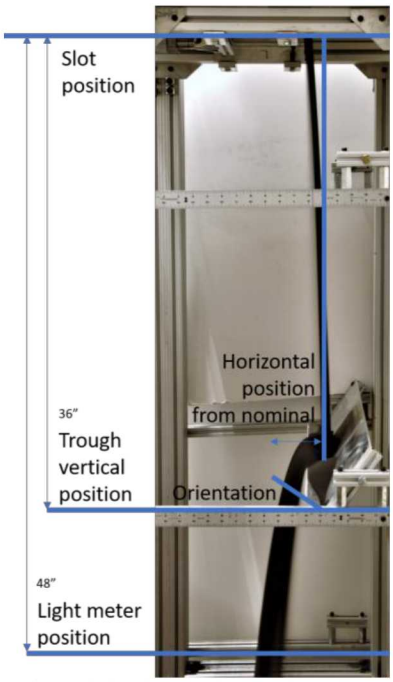

FIGURE 5: Selected single 90° internal angle trough test: 36" vertical position, nominal horizontal position, 35° orientation angle, and 1/2" slot depth or 5.8 kg s^{-1} m^{-1} particle mass flow rate

Selected particle pile profiles are shown for a trough at 12" vertical position and 45° orientation angle for different horizontal position in Figure 6. In Figure 6a, the trough is positioned slightly forward of the nominal position. In this position, particles appear to bounce off the front of the particle pile in the trough and over the trough leading edge. This bouncing results in more z direction curtain spread below the trough compared to the other horizontal positions shown in Figure 5 (nominal position), Figure 6b (1" forward from nominal), and Figure 6c (2" forward from nominal). For positions forward from nominal, falling particles appear to impact the particle pile and undergo a combination of the following: (1) roll forward and off the trough or (2) lodge in the pile and push other stationary particles forward and off the trough.

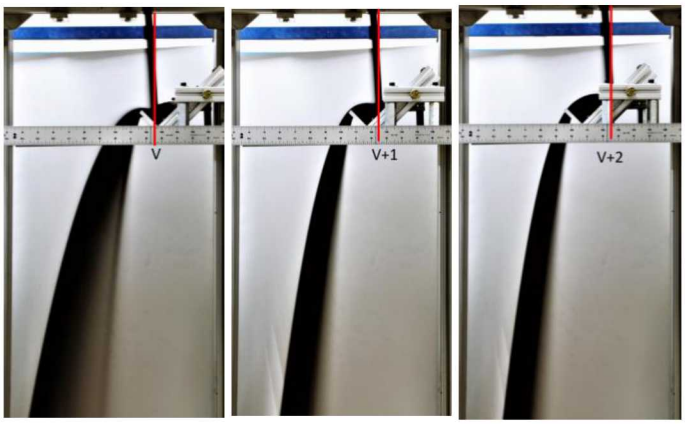

(a) (b) (c)

FIGURE 6: Selected particle piles images in 90° internal angle troughs positioned vertically 12" from the slot, at a 45° orientation, 1/2" slot depth or 5.0 kg s^{-1} m^{-1} particle mass flow rate, with horizontal position: (a) back from nominal position (0" from trough vertex or "V"), (b) 1" forward from nominal position, and (c) 2" forward from nominal position

Selected particle pile profiles are shown for a trough at 36" vertical position and 1" forward from the nominal horizontal position for different orientation angles in Figure 7. The size of the particle pile increases with increasing orientation angle; however, there is no discernable different between the particle behavior leaving the trough for different orientation angles in the images. Size of the particle pile in the troughs has the potential to influence trough and local particle temperatures in a falling particle receiver. Additional particles in the troughs will further shade the trough from direct irradiation, and the additional thermal mass has the potential to insulate the trough back edge from high temperature, directly irradiated particles. Thermal analysis is warranted.

(a) (b) (c) (d)

FIGURE 7: Selected profile images of particle piles in 90° internal angle troughs positioned vertically 36" from the slot, horizontal position 1" forward from the nominal position, 1/2" slot depth or 5.8 kg s^{-1} m^{-1} particle mass flow rate, with orientation angle: (a) 35°, (b) 45°, (c), 55°, and (d) 65°

Particle curtain transmissivity versus horizontal position is shown in Figure 8 for three trough vertical positions and four trough orientations. Note the different y axis scale in Figure 8a and Figure 8b. For the 1/4" slot depth results, the slot depth was not adjusted between all results for troughs at 12" and 24" vertical position, with measured particle mass flow rates of 0.599 and 0.588 kg s^{-1}, respectively or 2.0 and 1.9 kg s^{-1} m^{-1}, respectively. Results for troughs at 36" vertical position had a particle linear mass flow rate of 2.0 kg s^{-1} m^{-1}. For the 1/2" slot depth results, the slot depth was not adjusted between all results for troughs at 12" and 24" vertical position. All 12" and 24" vertical position results were obtained on the same day with one particle mass flow rate measurement or 1.53 kg s^{-1} or 5.0 kg s^{-1} m^{-1}. Results for troughs at 36" vertical position had a particle linear mass flow rate of 5.8 kg s^{-1} m^{-1}.

For 1/4" slot depth, transmissivity generally decreases with increasing vertical and decreasing horizontal positions. Increasing horizontal position results in the particle curtain impinging on the back edge of the trough and larger the particle piles. Particle-to-trough contact could result in more particle bouncing, lower particle volume fraction, and higher curtain transmissivity. For 1/2" slot depth, transmissivity is generally lower for 24" vertical position and 1" forward from nominal horizontal position with a few exceptions. Greater particle velocity and z direction curtain spread after a drop distance of 24" has the potential to interact with the particle pile differently than the lower particle velocities after a drop distance of 12". The change in trends between 12" and 24" vertical positions suggests that the curtains impinging on larger particle piles result in particles exiting the trough with lower velocity and higher particle volume fraction for higher particle curtain velocities at impact.

For both slot depths, particle curtain transmissivity does not appear strongly correlated to trough orientation for 24" and 36" vertical positions. For the 12" vertical position, transmissivity generally decreases with increasing orientation with a few exceptions. Of the considered vertical positions, the particle velocity is lowest at 12" compared to 24" and 36". At lower velocities, we hypothesize particle pile effects have more of an influence on particle trough exit behavior than particle bouncing effects which have more of an influence at higher particle velocities.

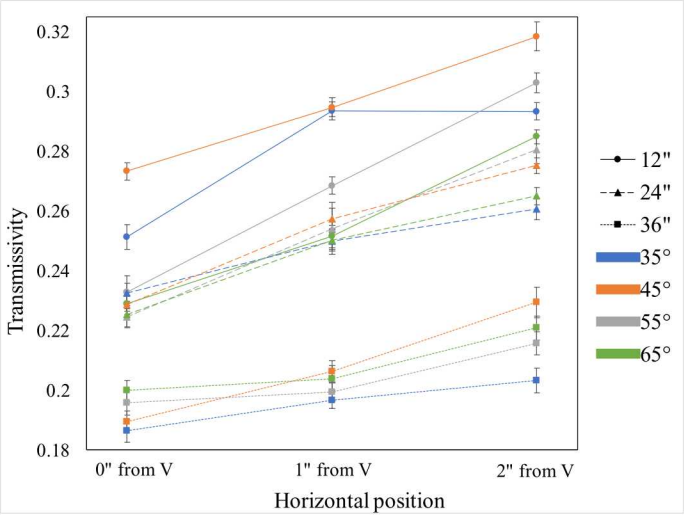

(a)

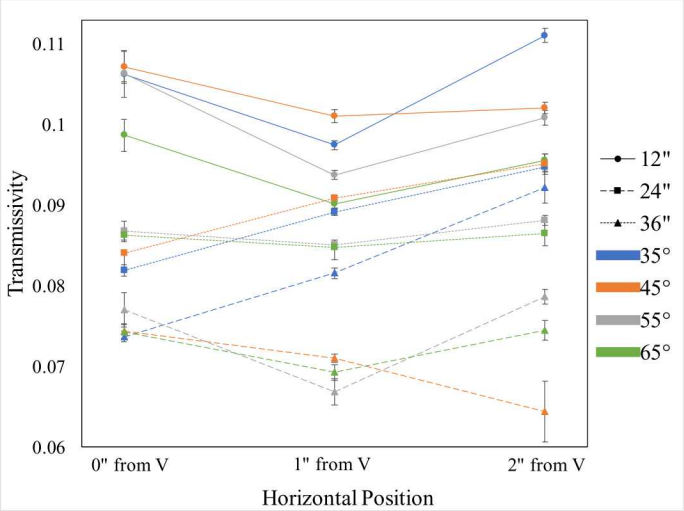

(b)

FIGURE 8: Particle curtain transmissivity versus 90° internal angle trough horizontal position for slot depth (a) 1/4" and (b) 1/2" for various trough vertical positions and orientations; error bars represent the aggregated standard deviation of measured values

The results with 90° internal angle troughs will next be compared to the baseline results. For 1/4" slot depth, all configurations at 12" vertical position (light meter positioned at 24" below the slot) yielded curtains with comparable transmissivity values as the baseline curtain measured at 24". For configurations at 24" vertical position (light meter positioned at 36"), transmissivity decreased from 0.34 in the baseline case to roughly 0.24–0.25 for all configurations with troughs. For configurations at 36" vertical position (light meter positioned at 48"), transmissivity improves even more over the baseline case at 48": from 0.4 in the baseline case to roughly 0.2 in configurations with troughs at 36" vertical position. Thus, troughs improved curtain transmissivity over the baseline curtain when the trough horizontal position was greater than 12".

For 1/2" slot depth, all configurations at 12" vertical position yielded curtains with higher transmissivity values than the baseline curtain at 24"; transmissivity increased from 0.06 in the baseline case to roughly 0.1 in cases with troughs. All configurations at 24" vertical position yielded curtains with comparable transmissivity values as the baseline curtain measured at 36". For configurations at 36" vertical position, transmissivity decreased slightly from 0.1 in the baseline case to roughly 0.08–0.09 for all configurations with troughs. Thus, troughs improved curtain transmissivity over the basline curtain when the trough horizontal position was greater than 24". For larger particle linear mass flow rates, the drop distance before troughs improve curtain transmissivity is greater, because the curtain is thicker and loses opacity at a lower rate than thin curtains.

2.3 Single trough with 120° internal angle

To investigate the influence of trough internal angle on transmissivity, the test campaign for the single trough with 90° internal angle was repeated with a single trough with 120° internal angle. Selected particle pile images are shown in Figure 9 for 24" vertical position and 25° orientation for varying horizontal position. The particle piles are much larger than those observed for 90° internal angle troughs at 35° orientation (see Figure 5). However, the particle trajectory leaving the trough and z direction curtain spread look similar for the same trough position and orientation for both 90° and 120° internal angle troughs.

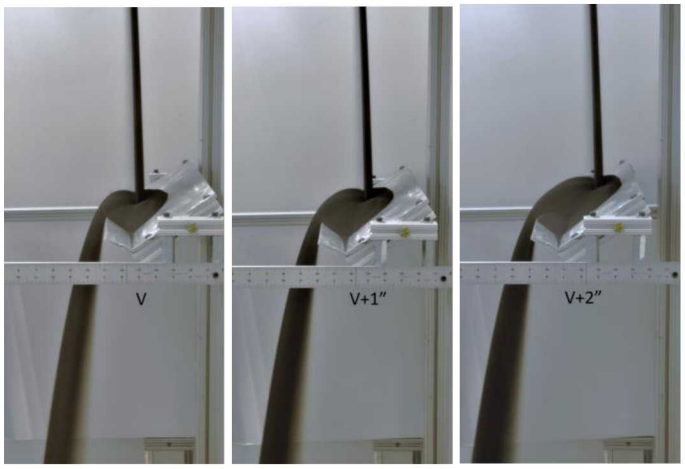

(a) (b) (c)

FIGURE 9: Selected profile images of particle piles in 120° internal angle troughs positioned vertically 24" from the slot at a 25° orientation, 1/2" slot depth or 5.1 kg s^{-1} m^{-1} particle linear mass flow rate, with horizontal position: (a) nominal position (0" from trough vertex or "V"), (b) 1" forward from nominal position, and (c) 2" forward from nominal position

Particle curtain transmissivity versus trough horizontal position is shown in Figure 10 for two trough vertical positions and three trough orientations for slot depths 1/4" and 1/2". Results for slot depth 1/4" all had a measured particle mass flow

rate of 0.594 kg s–1 or 1.9 kg s^{-1} m^{-1}. Results for slot depth 1/2" all had a measured particle mass flow rate of 1.55 kg s^{-1} or 5.1 kg s^{-1} m^{-1}.

Data points are limited due to physical limits of the test apparatus and troughs. The back of the frame limits the position of the back edge of a trough, and the particle curtain slot horizontal position is fixed 8" forward from the back frame. Large orientation angles and horizontal positions towards the back of the frame (particle curtain impinging toward the vertex of the trough) cannot be accommodated for 120° internal angle troughs, because the back edge of a 120° internal angle trough extends further than the back edge of a 90° internal angle trough for the same trough orientation and horizontal position. Future work may include cutting trough back edge corners to allow a greater range of positions. Large orientation angles (greater than 45°), horizontal positions forward from the back of the frame (particle curtain impinging behind the vertex of the trough), and higher particle mass flow rates are also limited for 120° internal angle troughs, because large orientation angles can result in particles falling over the back edge of the trough rather than the front. In Figure 9c, the particle pile is approaching the back of the trough back edge; at larger orientation angles, the pile will reach up to the edge and flow over the back side. Trough back edges can be extended to prevent particles from falling over the back edge, however, this compounds the position limitation imposed by the back of the frame. All possible positions from the previous test campaign without particles falling over the trough back edge, plus an additional trough orientation value (25°), are reported.

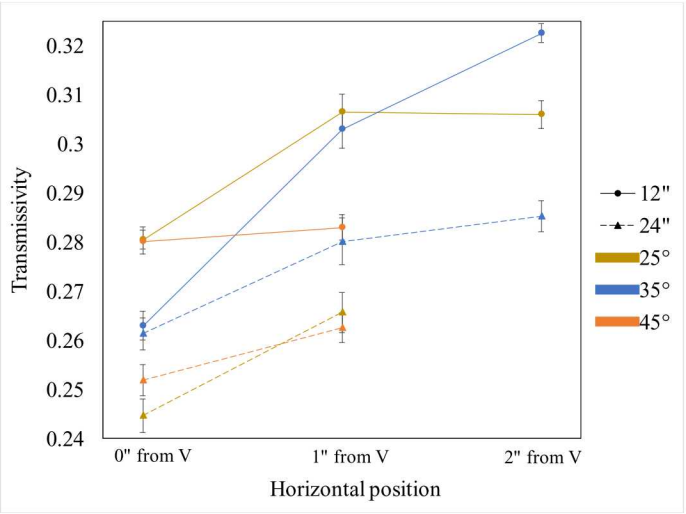

(a)

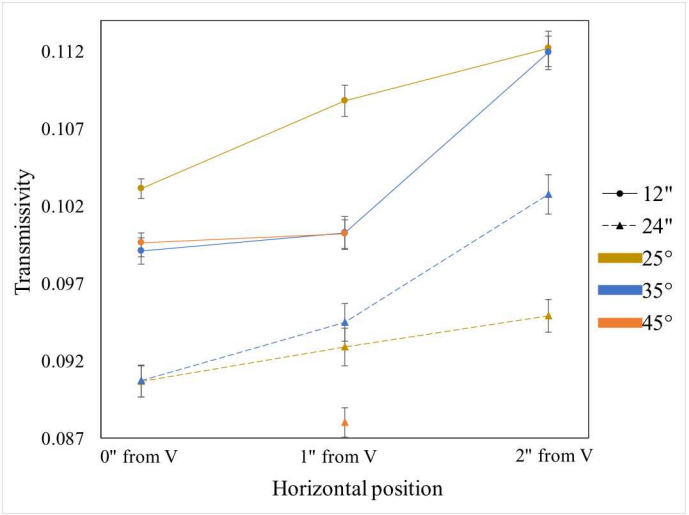

(b)

FIGURE 10: Particle curtain transmissivity versus 120° internal angle trough horizontal position for (a) 2.0 kg s^{-1} m^{-1} and (b) 5.1 kg s^{-1} m^{-1} particle mass flow rates for various trough vertical positions and orientations; error bars represent the aggregated standard deviation of measured values

Transmissivity decreases with increasing vertical position and decreasing horizontal position for both slot depths, similar to result for 90° internal angle troughs with 1/4" slot depth. No consistent trends are observed for transmissivity varying with orientation angle for either slot depth, similar to the results for 90° internal angle troughs with both considered slot depths.

Change in transmissivity with horizontal position for 120° internal angle troughs with 1/2" slot depth, shown in Figure 10b shows a different trend that change in transmissivity with horizontal position for 90° internal angle troughs with the same slot depth. For 90° internal angle trough results shown in Figure 8b, there are no consistent trends relating horizontal position to lowest transmissivity for a constant vertical position and orientation angle. For 120° internal angle trough results shown in Figure 10b, the nominal horizontal position resulted in the lowest transmissivity for a constant vertical position and orientation angle. We hypothesize that particle pile size varies substantially enough to affect transmissivity more than other considered variables in cases with 90° internal angle troughs, while particle pile size is always larger in cases with 120° internal angle troughs and does not affect transmissivity as much as other considered variables.

Results with 120° internal angle troughs will next be compared to the baseline curtain results. For 1/4" slot depth, configurations with 12" and 24" vertical position2 result in curtains with higher and lower transmissivity, respectively compared to the analogous baseline curtain transmissivity. For 1/2" slot depth, all considered configurations perform worse than the baseline curtain.

Trough configuration for 120° internal angle troughs cannot be optimized as well as for 90° internal angle troughs due to the limitations of the test apparatus. Troughs with larger internal

angles have the potential to perform better in real receivers, because the large curtain acceptance area accommodates particle curtain motion due to transient effects. Larger acceptance area can also be achieved with 90° internal angle troughs with longer back edge lengths.

2.4 Two troughs with 90° internal angle

Based on results for 90° and 120° internal angle troughs, 90° internal angle troughs were selected to be investigated further. A first trough is fixed at 12" vertical position, 65° orientation, and in the nominal horizontal position, and a second trough is added. A vertical position of 12" below the slot was selected for the first trough to maximize distance below the first trough; 65° orientation and the nominal horizontal position were selected because that configuration yielded the lowest transmissivity for 12" vertical position troughs. For the second trough, vertical position 12" and 24" below the first trough are considered as well as orientations angles from 35–65° and horizontal positions from nominal to 2" forward from nominal. Only 1/4" slot depth was considered because of the limited vertical distance of the test apparatus for larger slot depths as previously discussed.

Results are shown in Figure 11. Generally, the second trough positioned 24" below the first results in lower transmissivities than those positioned 12" below the first trough. For the second trough positioned 12" below the first, horizontal positions towards the nominal position and decreasing orientation angles result in lower transmissivities, while for the second trough positioned 24" below the first, there are no consistent trends in transmissivity with varying horizontal position or orientation angle.

Transmissivity values for a second 90° internal angle trough 12" below the first span a similar range to values for a single 90° internal angle trough 12" below the slot. This similarity shows that troughs can have 'resetting effect' on particle curtain transmissivity.

All configurations with two troughs result in transmissivities lower than baseline values. For a second trough 12" below the first, the light meter is 36" below slot. The baseline curtain transmissivity for this slot depth at 36" is 0.34, while results with two troughs range from 0.24–0.30. For a second trough 24" below the first, the light meter is 48" below slot. The baseline curtain transmissivity at 48" is 0.4, while results with two troughs range from 0.21–0.25. For two troughs, non-optimized configurations still resulted in improved curtain transmissivity.

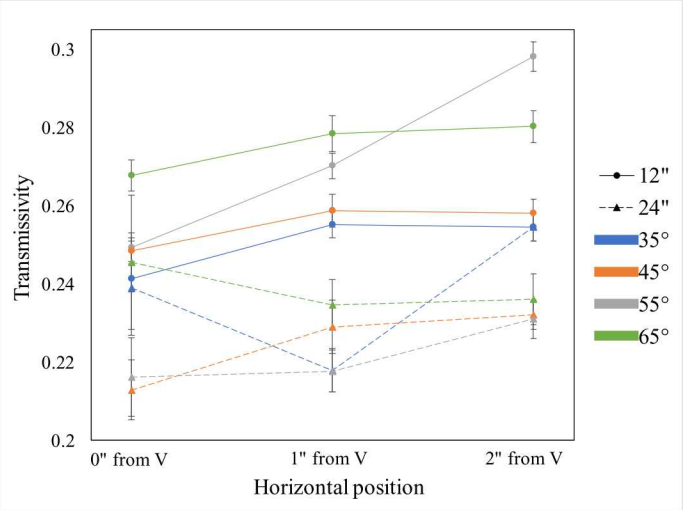

FIGURE 11: Particle curtain transmissivity versus 90° internal angle second trough horizontal position for 2.1 kg s^{-1} m^{-1} particle mass flow rate for various second trough vertical positions and orientations; error bars represent aggregated standard deviation of measured values

CONCLUSIONS AND FUTURE WORK

Certain configurations decrease transmissivity compared to baseline values. The particle curtain does not leave the troughs with as low a horizontal velocity as when it leaves the slot, as shown by the different path trajectories: baseline curtain travels mostly downward with some negative z direction velocity, while particle curtains leaving the troughs travel downward and forward with positive z direction velocity of a greater magnitude than the negative z direction velocity in the baseline case. The particle curtain has a higher initial opacity when exiting the slot than when leaving the troughs. Thus, there is a minimum height the curtain must fall before introduction of troughs will improve opacity.

Trough horizontal position and, to a lesser extent, orientation affect curtain transmissivity, suggesting particle pile size and shape and the position the particle curtain impinges on the pile influence how particles exiting the trough. Curtain transmissivity decreases with increasing trough orientation angle for troughs placed closer to the slot, suggesting larger particle piles in the troughs lead to less particle bouncing caused by less particle-to-trough contact.

A unique optimized trough geometry and configuration likely exists for a given particle linear mass flow rate and drop distance. Vertical distance and particle mass flow rate have greater impact on trough performance than trough internal angle, horizontal position, and orientation. A single, fixed trough configuration that meets the minimum trough vertical distance for the lowest target mass flow rate then has the potential to provide improvements in curtain transmissivity over a free fall curtain for a range of particle linear mass flow rates. Non-optimal trough configurations should still be screened for all target particle mass flow rates to prevent selection of a

configuration that results in substantial particle bouncing and loss curtain opacity.

A major limitations of the current study is the temperature of the particles. Particle flow behavior is expected to change at temperatures typical of falling particle receivers: 500–700°C. Particles get stickier as temperature increase, and sticky particles could result in decreased bouncing, particles exiting the trough with lower positive z and negative y velocities, and/or particles exiting the trough with more random momentum.

Future cold flow testing with this test apparatus will include alternative trough designs/geometries, additional slot depths, and investigation of lateral particle curtain opacity variations. To investigate edge effects, the light meter will be moved in the positive and negative y directions along width of curtain and the curtain width will be increased from 12" to 18".

The StAIR concept has been investigated numerically using computational fluid dynamics in a 1 MW_{th} falling particle cavity receiver [10]. The StAIR concept decreases particle velocity which, in a receiver, was found to decrease advective loss of hot air out of the open aperture. The StAIR concept was also found to decrease receiver back wall temperatures, which can limit operating conditions. Decreased back wall temperatures allow a higher solar flux operating envelope which has the potential to increase receiver thermal efficiency.

This study and the numerical investigations of the StAIR concept will be used to design an angle iron-based multistage release system for installation in an existing 1 MW_{th} falling particle receiver [4][7][9] at the National Solar Thermal Test Facility at Sandia National Laboratories in Albuquerque, NM and tested on sun in 2020.

ACKNOWLEDGEMENTS

The authors gratefully acknowledge Lam Banh and Kevin Good of Sandia National Laboratories for assistance with the design and fabrication of the test rig; Luis Garcia Maldonado of Sandia National Laboratories for assistance with LabVIEW programming; and Roger Buck of Sandia National Laboratories for assistance with the linear actuator installation.

This work was funded in part or whole by the U.S. Department of Energy Solar Energy Technologies Office under Award Number 34211. This report was prepared as an account of work sponsored by an agency of the United States Government. Neither the United States Government nor any agency thereof, nor any of their employees, makes any warranty, express or implied, or assumes any legal liability or responsibility for the accuracy, completeness, or usefulness of any information, apparatus, product, or process disclosed, or represents that its use would not infringe privately owned rights. References herein to any specific commercial product, process, or service by trade name, trademark, manufacturer, or otherwise does not necessarily constitute or imply its endorsement, recommendation, or favoring by the United States Government or any agency thereof. The views and opinions of the authors expressed herein do not necessarily state or reflect those of the United States Government or any agency thereof.

Sandia National Laboratories is a multimission laboratory managed and operated by National Technology and Engineering Solutions of Sandia, LLC., a wholly owned subsidiary of Honeywell International, Inc., for the U.S. Department of Energy's National Nuclear Security Administration under contract DE-NA0003525.

REFERENCES

[1] Hruby, J. M. and Steele, B. R. *Chemical Engineering Progress*, 1986

[2] Ho, C. K. *Applied Thermal Engineering*, 2016

[3] Kim, K, Siegel, N., Kolb, G., Rangaswamy, V., and Moujaes, S. F. *Solar Energy*, 2009

[4] Ho. C. K., Christian, J. M., Romano, D., Yellowhair, J., Siegel, N., Savoldi, L., and Zanino, R. *Journal of Solar Energy Engineering—Transactions of the ASME*, 2017.

[5] Kumar, A., Kim, J., and Lipiński, W. *Journal of Solar Energy Engineering—Transactions of the ASME*, 2018.

[6] Lee, T., Lim, S., Shin, S., Sadowski, D., Abdel-Khalik, S., Jeter, S., and Al-Ansary, H. *Solar Energy*, 2015.

[7] Ho, C. K., Christian, J., Yellowhair, J., Armijo, K., Kolb, W., Jeter, S., Golob, M., Nguyen, C. *Journal of Solar Energy Engineering—Transactions of the ASME*, 2019.

[8] Kim, J., Kumar, A., Gardner, W., and Lipiński, W. *AIP Conference Proceedings*, 2019.

[9] Ho, C. K., Peacock, G., Christian, J. M., Albrecht, K., Yellowhair, J. E., and Ray, D. *AIP Conference Proceedings*, 2019.

[10] Shaeffer, R., Mills, B., Yue, L., and Ho, C. K. *Proceedings of the ASME 2020 14th International Conference on Energy Sustainability*, Denver, CO USA, June 8–10, 2020.